

1 **Climate simulations and pollen data reveal the distribution**
2 **and connectivity of temperate tree populations in eastern**
3 **Asia during the Last Glacial Maximum**

4 Suzanne Alice Ghislaine Leroy ^{1*}, Klaus Arpe ^{2*}, Uwe Mikolajewicz³, and Jing Wu ⁴

5 1) Aix Marseille Univ, CNRS, Minist Culture, LAMPEA, UMR 7269, 5 rue du Château de l'Horloge, BP
6 647, 13094 Aix-en-Provence Cedex 2, France

7 2) Max-Planck-Institute for Meteorology, Hamburg, Germany, retired

8 3) Max-Planck-Institute for Meteorology, Hamburg, Germany

9 4) Institute of Geology and Geophysics, Chinese Academy of Science (IGGCAS)

10 Beijing, 100029, P. R. China

11
12 * corresponding author

13 klaus.arpe@mpimet.mpg.de leroy@msh.univ-aix.fr,

14 **ABSTRACT**

15 Publications on temperate deciduous tree refugia in Europe are abundant, but little is known about
16 the patterns of temperate tree refugia in eastern Asia, an area where biodiversity survived
17 Quaternary glaciations and which has the world's most diverse temperate flora. Our goal is to
18 compare climate model simulations with pollen data in order to establish the location of glacial
19 refugia during the Last Glacial Maximum (LGM) period. Limits in which temperate deciduous
20 trees can survive are taken from the literature. The model outputs are first tested for the present by
21 comparing climate models with published modern pollen data. As this method turned out to be
22 satisfactory for the present, the same approach was used for the LGM, Climate model simulations
23 (ECHAM5 T106), statistically further down-scaled, are used to infer the temperate deciduous trees
24 distribution during the LGM. These were compared with available fossil temperate tree pollen
25 occurrences.

26

27 The impact of the LGM on the eastern Asia climate was much weaker than on the European
28 climate. The area of possible tree growth shifts only by about 2° to the south between the present
29 and the LGM. This contributes to explain the greater biodiversity of forests in eastern Asia
30 compared to Europe. Climate simulations and the available, although fractional, fossil pollen data
31 agree. Therefore, climate estimations can safely be used to fill areas without pollen data by
32 mapping potential refugia distributions. The results show two important areas with population
33 connectivity: The Yellow Sea emerged shelf and the southern Himalayas. These two areas were
34 suitable for temperate deciduous tree growth, providing corridors for population migration and
35 connectivity (i.e. less population fragmentation) in glacial periods. Many tree populations live in
36 interglacial refugia; not glacial ones. The fact that the model simulation for the LGM fits so well
37 with observed pollen distribution is another indication that the used model is good to simulate also
38 the LGM period.

39 **Key words**

40 Eastern Asia, ECHAM5 model, Last Glacial Maximum, pollen, temperate deciduous trees,
41 population connectivity

42 **Supplementary information** is added, discussing **Appendix S1: Monsoon progression in the model**
43 **compared to observation**
44 **and**
45 **Appendix S2: Uncertainty of precipitation analysis**

46

47 **Introduction** Eastern Asia temperate deciduous forests boast the world's most diverse temperate
48 deciduous forest flora (Donoghue and Smith, 2004; Qiu et al., 2011). They also contain the highest
49 numbers of Tertiary relict taxa that have disappeared from Europe (Milne and Abbott, 2002;
50 Svenning, 2003), such as *Carya* and *Parrotia* (Li and Del Tredici, 2008; Orain et al., 2013). The
51 reason for this situation should be sought in the history of these forests through Quaternary
52 glaciations and earlier. The last time when these forests had a considerable reduction of their

53 population or underwent a shift of their distribution was during the Last Glacial Maximum (LGM),
54 i.e. 21,000 years ago. On different continents, this happened in different ways due to the climate of
55 the area, the topography (including the orientation of the main mountain ranges that may act as
56 geographical corridors or barriers), the location and extent of icecaps and the extent of emerged
57 coastal shelves. In Europe, during the LGM, the temperate deciduous forests, especially the warm-
58 temperate tree species, died out in much of northern and central Europe and survived in refugia in
59 the mountainous areas of the three southern peninsulas: Iberia, Italy and the Balkans, as well as in
60 some smaller areas around the Black Sea and the southern Caspian Sea (Leroy and Arpe, 2007;
61 Arpe et al., 2011).

62 Various methods have been used to establish the locations of glacial refugia of temperate
63 deciduous trees during the LGM in Eastern Asia. For example, population distributions have been
64 published based on phylogenetic data in Eastern Asia (Qian and Ricklefs, 2000) and based on
65 biomisation using palaeo-data for the Japanese archipelago (Takahara et al., 2000; Gotanda and
66 Yasuda, 2008) and for China (Harrison et al., 2001). A disagreement regarding the location of
67 temperate tree refugia in China, especially at its northern limit, has appeared: Harrison et al. (2001)
68 proposed the northern limit of the temperate deciduous forest biome to have retreated far south
69 (south of 35° N) versus Qian and Ricklefs (2000) who suggested an extension of the temperate
70 forest over the emerged continental shelf. Qian and Ricklefs (2000) highlighted the important role
71 played by physiography heterogeneity, climatic change and sea-level changes in allopatric
72 speciation. According to the results of their ecological analysis, a temperate tree population
73 extended across the emerged shelf and linked populations in China, Korea and Japan during glacial
74 times. This led to the concept of interglacial fragmentation and refugia.

75 Additional information from phylogenetics of temperate deciduous trees should also be considered
76 for phylogeography purposes. But few trees/bushes belonging to the deciduous forest have been
77 analysed so far. A temperate deciduous bush, *Ostryopsis davidiana*, indicates multiple LGM
78 refugia both south and north of the Qin Mountains (Tian *et al.*, 2009).

79 To be complete, it should be mentioned that the distribution of key temperate tree biomes (discrete
80 points) for the LGM can be found in Ni et al. (2014).

81 Our aim is to contribute to this debate on the northern limit of temperate deciduous trees by using
82 another approach to ecology, to biomes and to phylogeography: i.e one based on climate
83 model simulations. The results from this approach are validated by pollen data, whose amount has
84 increased spectacularly since 2010. Distribution maps are then produced.

85 **2 MATERIAL AND METHODS**

86 The climatic data, model and methods used in this study are described by Leroy and Arpe (2007)
87 and Arpe *et al.* (2011) in more detail. Coupled ECHAM5-MPIOM atmosphere ocean model
88 simulations were carried out, though with a very low horizontal resolution of T31 (i.e. a spectral
89 representation which resolves waves down to 31 on any great circle on the earth
90 corresponding to approx. 3.75°). In such a coupled model, the atmosphere as well as the ocean
91 and the vegetation were simulated and interact with each other and generated their own Sea
92 Surface Temperature (SST) and vegetation parameters. These SSTs and vegetation parameters
93 were then used for uncoupled ECHAM5 T106 atmospheric simulations. The ECHAM models
94 including the coupled ocean model were developed at the Max-Planck Institute for Meteorology in
95 Hamburg (MPI).

96 The models were run on one hand with the present-day conditions concerning the orography, solar
97 radiation, ice cover and CO₂ and on the other hand under LGM conditions concerning the same
98 parameters (e.g. atmospheric CO₂ concentration at 185 ppm). The simulations for the present and
99 the LGM with a T106 resolution (approx. 1.125° horizontal resolution) model with 39 atmospheric
100 vertical levels were carried out with the ECHAM5 atmospheric model (Roeckner et al., 2003). The
101 boundary data, e.g. the SST and vegetation parameters, were taken from the coupled ECHAM5-
102 MPIOM atmosphere ocean dynamic vegetation model (Mikolajewicz et al., 2007) simulations,
103 which have been made for the present and the LGM with a spectral resolution of T31 and 19

104 vertical levels. The experimental setup is largely consistent with the Paleoclimate Modelling
105 Intercomparison Project phase 2 PMIP2 (Braconnot et al., 2007). These SSTs were corrected for
106 systematic errors of the coupled run by adding the SST differences between observed SSTs and
107 simulated ones for the present, the corrections are generally below 3°C.

108 In Arpe et al. (2011), comparisons of the model generated SSTs with other reconstructions, e.g.
109 from the MARGO project (Kucera et al., 2005), were performed and good agreement was found.
110 Differences to the CLIMAP (1981) reconstruction agree with findings by PMIP2 (Braconnot et al.,
111 2007). Also, other information from the LGM gave further confidence in the performance of the
112 model. In Arpe et al. (2011), the importance of a high resolution is stressed. Therefore, we use here
113 again the T106 model. Intuitively one assumes that the model that provides good estimations for
114 the present climate would also be best for simulating a climate with a different external forcing
115 such as during the LGM. Indeed Arpe et al. (2011) found good correspondence between pollen
116 findings for the LGM and the estimation of possible tree growth for Europe, which increased
117 confidence in that model. As the climate of Eastern Asia is quite different to that of Europe, we try
118 to find further evidence for the high performance of the model in Eastern Asia.

119 It is generally assumed that results from model simulations become more robust when using an
120 ensemble of different model simulations; but we did not do that. As the ECHAM models have been
121 shown by Reichler and Kim (2008) to belong to the best ones and by including other ones, we
122 would only dilute our results because of very different results in different simulations (Tian and
123 Jiang,(2016). Further, most of the available simulations are of much lower resolution than T106,
124 that used here, and which we believe is essential for a region of diverse topography such as Eastern
125 Asia. When combining the results of different models, an interpolation to a common grid is
126 inevitable and that creates some smoothing with a further loss of resolution.

127 Nevertheless, even a T106 model resolution might not be sufficient for our investigation. Kim et al.
128 (2008) demonstrate the importance of a high resolution with their model, among others, for the
129 response of the Eastern Asian summer monsoon under LGM conditions. Therefore, we did a down-

130 scaling to a 0.5° resolution. For that, the differences between the model simulations for the LGM
131 and the present are added to a high-resolution present-day climatology. The climatology that
132 seemed best for our investigation is that of Cramer and Leemans (Leemans, R. and Cramer (1991) ;
133 Cramer, 1996), below abbreviated as “C&L”. With this method, the impact of possible systematic
134 errors of the model is reduced. This method works only if the simulations are already reasonable;
135 otherwise it might happen that e.g. negative precipitation amounts may occur. We could use this
136 method only for the precipitation and 2m air temperature (T2m) while the winds had to be taken
137 directly from the model simulations.

138 To improve the understanding of limitations in the climate data, estimates of the present
139 climatology with data from the Global Precipitation Climate Center (GPCC) (Schneider et al.,
140 2011; Becker et al., 2013; GPCC, 2013) and with data from the ECMWF interim reanalyses (ERA)
141 (Dee et al., 2011; ECMWF, 2014) are used.

142 Lower CO₂ concentration in the atmosphere during the LGM has caused a decline of pollen
143 production. Therefore, low pollen concentrations or influxes may already be indicative of the
144 presence of trees (Ziska and Caulfield, 2000; Leroy, 2007). It should be noted that we are here not
145 working at the level of forests, nor of biomes. Hence it is considered that pollen sites will reliably
146 indicate the survival of temperate deciduous trees (summer-green and broadleaf), if records have a
147 sub-continuous curve of at least one temperate taxon such as deciduous *Quercus*, *Ulmus*, *Carpinus*
148 or *Tilia*. The study focuses on the period of the LGM, hence on an age of 21± 2 cal ka BP (Mix et
149 al., 2001). The geographical areas of China, Japan, SE Russia, Korea and the Himalayas are
150 explored. The dataset includes terrestrial and marine sites. A literature review of pollen data was
151 made. It was first based on the large compilations of Cao et al. (2013) mainly for China and of
152 Gotanda and Yasuda (2008) for Japan. Then this was enlarged geographically and with an update
153 including more recent publications.

154 Modern pollen assemblages were used to check the validity of the tree growth limits chosen. The
155 following databases were used: Zheng et al. (2014) for China and Gotanda et al. (2002) for Japan.

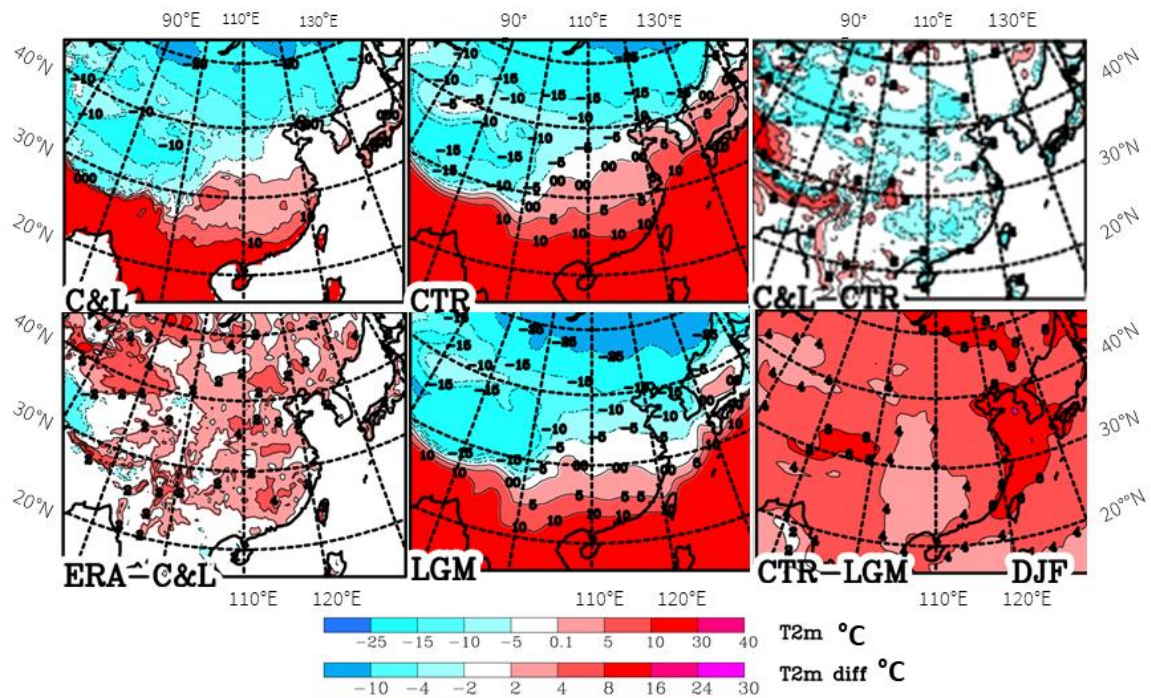
156 This was complemented by local studies such as by Park (2011) and Park and Park (2015) for
157 Korea and the Himalayas (Fuji and Sakai, 2002; Chung et al., 2010; Kotlia et al., 2010; Yi and
158 Kim, 2010). It was not aimed to be exhaustive. From these databases, the occurrences of temperate
159 deciduous trees (mainly deciduous *Quercus*, and *Ulmus*, but also others such as *Carya*, *Tilia*,
160 *Carpinus*) of at least 0.5% were selected.

161 **3 CLIMATE OF EASTERN ASIA**

162 In our earlier investigations on glacial refugia of trees over Europe (Leroy and Arpe 2007; Arpe et
163 al., 2011), limiting factors for possible tree growth were the precipitation during summer, the mean
164 temperature of the coldest months and the growing degree days (number of days with temperatures
165 $>5^{\circ}\text{C}$) (GDD5), the latter is related to the summer temperatures. The climate of Eastern Asia is
166 different to that of Europe and a short review of its climate is therefore needed in order to adapt the
167 limits.

168 The climate of Eastern Asia is dominated by the monsoon (more information in Appendix S1 of
169 Supporting Information) as well as by its very strong topographic variability. The latter makes it
170 difficult to create a reliable climatology on a regular grid. This is demonstrated for air temperature
171 T2m) during December to February (DJF) by comparing the C&L climatology with a long-term
172 mean from the ECMWF interim reanalysis (Dee et al. 2011; ECMWF-ERA. 2019) (ERA), a
173 simulation for the present (CTR) and LGM simulations (Fig. 1).

174



176

177 Fig. 1: Climatological mean distribution of T2m over Eastern Asia for December to February
 178 (DJF)

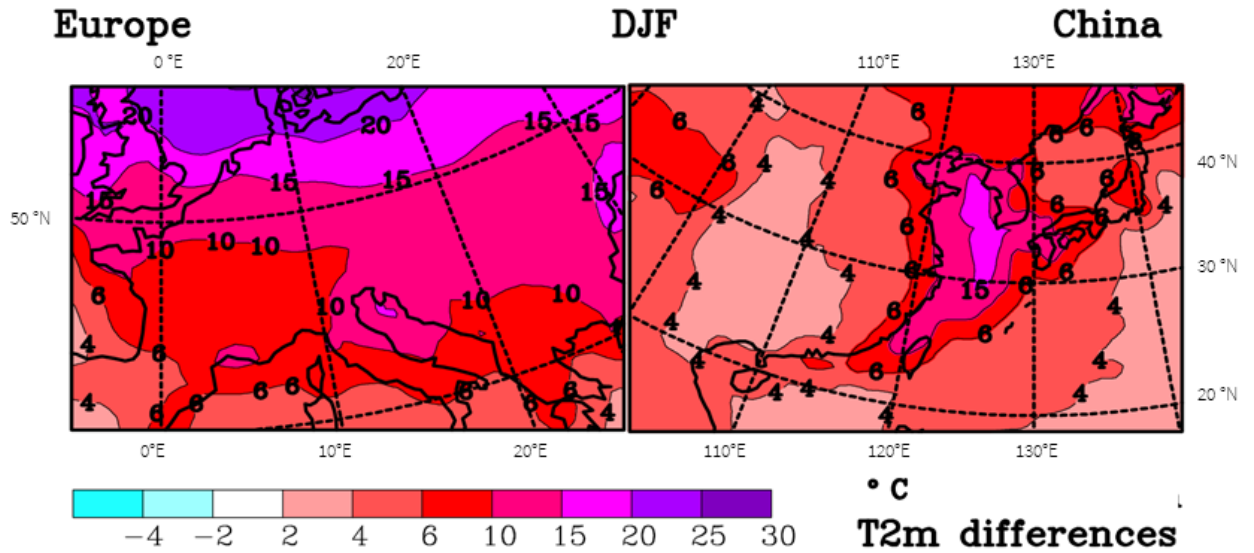
179 Values by Leemans, R. and Cramer (1991) (C&L), the ECMWF reanalysis (ERA) and model
 180 simulations (CTR and LGM), as well as some differences between them.

181 Much stronger structures in the C&L climatology compared to the other climatologies can be seen
 182 (Fig. 1). Moreover substantial differences are observed, e.g. the white band (-5 to 0°C) is
 183 positioned about 5° further north in eastern Asia in ERA compared to C&L with up to 4 °C warmer
 184 temperatures over a large part of Eastern Asia (Fig. 1, panel ERA- C&L). For the Caspian region,
 185 Molavi-Arabshahi et al. (2015) showed how biases of several °C in ERA can occur in mountainous
 186 areas when the topographic height in the ECMWF model and the real topography are different. So
 187 it is assumed that the warmer temperatures in ERA compared to C&L are due to this analysis
 188 system. The climate simulation for the present (Fig. 1, CTR) agrees similarly well with ERA and
 189 C&L, a little warmer than C&L and cooler than ERA (not shown).

190 A main purpose of different simulation periods (Fig. 1) is the display of changes from the LGM to
191 the present (Fig. 1 lower right). Over the Yellow Sea, temperatures differ by up to 16 °C, as a large
192 area of the ocean shelf emerged during the LGM, while the differences are much smaller for
193 continental China, mainly 4 to 5 °C. These changes between the present and the LGM are overall
194 much weaker than for Europe in winter (Fig. 2). Typical differences for continental central Europe
195 are 8-15 °C while they are only around 4-5 °C for the Eastern Asian continent. One has to take into
196 account that China is further south than central Europe, the central latitudes in the European map
197 are 45 to 50 °N while for China they are 32 to 37 °N, which contributes to explain the large
198 differences in the temperature change. Also, the proximity of the Fennoscandian ice sheet is of
199 importance for the colder temperatures in Europe, as well the weakening of the Gulfstream, which
200 presently supplies Europe with warmer temperature. The strong temperature change over the
201 Yellow Sea is a consequence of the larger heat capacity of the ocean, which limits the winter-time
202 cooling under present-day conditions. At the LGM, this area was emerged due to the lower sea
203 level, which leads to much stronger winter-time cooling.

204

205



206

207 Fig. 2: Difference maps between simulated CTR and LGM T2m during winter (DJF) for Europe
 208 and Eastern Asia.

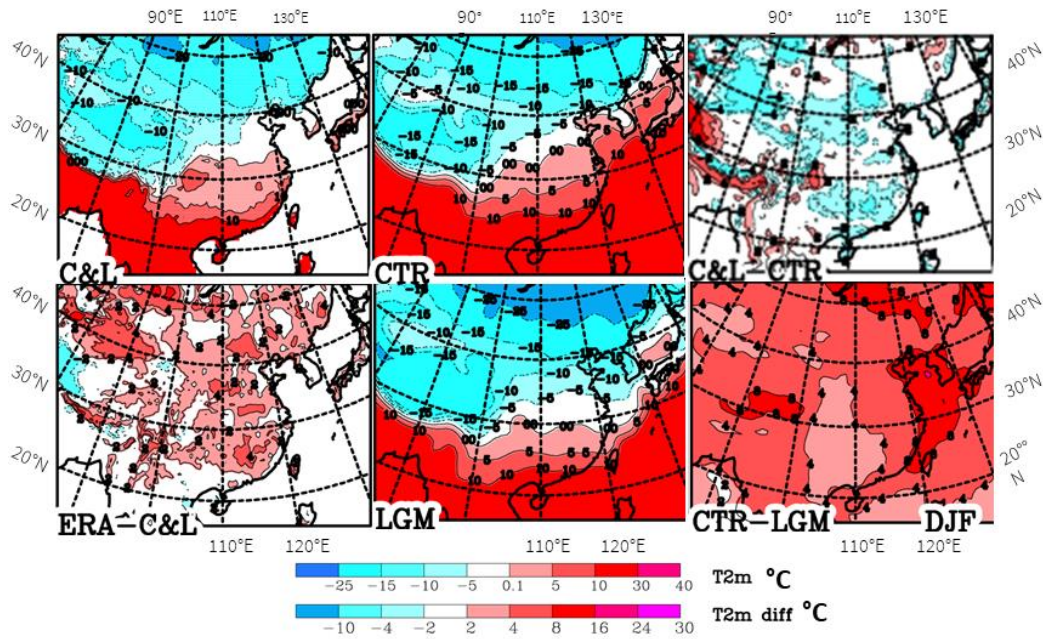
209

210 The summer temperatures are shown in Fig. 3. ERA temperatures are often warmer by around 2 °C
 211 than the ones in the C&L climatology (Fig. 3 lower left panel) the arguments for this difference
 212 given above for DJF apply here as well. The differences between the present and the LGM in the
 213 simulations increase from China's east coast of 2-3 °C to up to 6 °C over Tibet. This is similar to
 214 what Tian and Jiang (2016) found in PMIP3 simulations; they state that the temperature drop in the
 215 LGM is too low compared to proxy data. The summer temperatures are being used to calculate the
 216 GDD5. For the small changes shown here, we do not expect that GDD5 does impose much more
 217 limitation for the LGM than for the present for tree growth.

218

219

220



221

222 Fig. 3: Climatological mean distribution of temperature T2m (in °C) over Eastern Asia for June,

223 July August (JJA)

224 Values by Leemans, R. and Cramer (1991) (C&L), the ECMWF reanalysis (ERA) and model

225 simulations (CTR and LGM), as well as some differences between them.

226

227 The difference maps for CTR-LGM temperatures show values over the ocean (Figs. 1 to 3).

228 These differences may have an important impact on continental temperatures. Therefore, it is

229 interesting to compare these data with other estimates of the SST. For example, Annan and

230 Hargreaves (2013) show annual means of SST differences of around 2°C for the South China

231 Sea while our simulations have slightly larger values of 2.5 to 3°C, though this falls within the

232 uncertainty range given by Annan and Hargreaves (2013). A main difference is less cooling

233 during the LGM in our estimates at the Gulf and Kuroshio currents off the USA or Japan coast

234 (not shown as they are too far outside the area of interest).

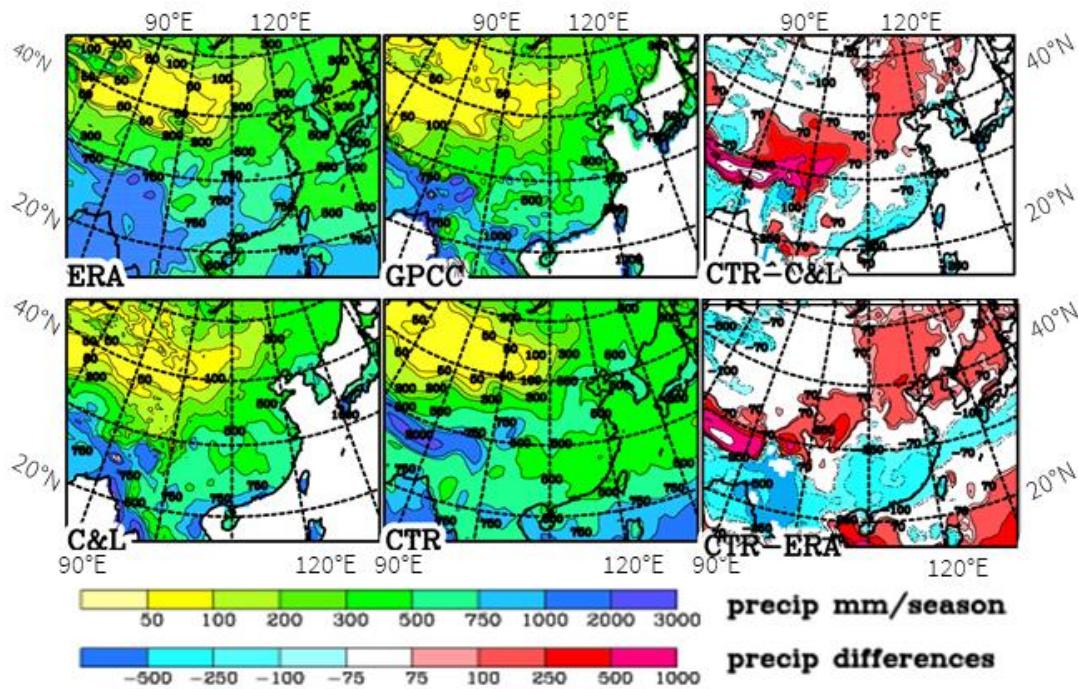
235 Summer precipitation is an important limiting factor for possible tree growth (Fig. 4). The sharp

236 gradient of precipitation along the southern slopes of the Himalayas in the three sets of analyses (the

237 climatology by C & L and the long-term means from ERA and GPCC) is clearly marked. The general
238 patterns agree in the three sets, though with some biases. C&L and GPCC agree best, probably;
239 because they are both based on precipitation observations at gauges. On the contrary, ERA is a model
240 product forced by a very large range and more evenly distributed observations; moreover ERA does
241 not use observed gauge precipitation. Differences between C&L and GPCC are mostly below 50
242 mm, especially in the northern areas where the precipitation is moderate. The differences between
243 C&L and ERA are also small in northern areas; but can become quite large where the amounts of
244 precipitation are large, mostly with ERA having larger precipitation amounts. The lower
245 precipitation rates in ERA for Korea and southern Japan in contrast to C&L and GPCC are
246 remarkable. Here the latter data are probably more accurate because this area is well-covered by
247 observations (Fig. S2.3) and the ERA model may not be able to resolve the strong topographic
248 structures. Many of the large uncertainties are probably due to the strong topographic structures over
249 Eastern Asia, which makes an analysis difficult and which is enhanced by a low density of
250 observational sites over western China (more information on precipitation accuracy in Appendix S2
251 of Supporting Information).

252 The systematic error of the model concerning China consists of the monsoon front being too far north
253 by 2° of latitude (Fig. S1.2) and with a too early northward propagation in the season (Appendix S1
254 of Supporting Information). As we only use the differences between the present and LGM this
255 systematic error is assumed to have only a minor impact on our results. Tian and Jiang (2016) found
256 a general weakening of the summer monsoon in PMIP3 simulations, especially a decrease of
257 precipitation in most of the simulations but they do not go into the details shown in Appendix S1 of
258 Supporting Information, which makes a comparison difficult. However, they noticed a large
259 variability within the models. For the area used in Fig. S1.2, they show a decrease of 10-20% of
260 summer precipitation in the LGM compared to the Control which agrees with our simulation,
261 strongest in June south of 32°N, though both CTR and LGM are too strong compared to ERA. In
262 our simulation, the strengthening north of 32°N for March to August for precipitation and 850 hPa
263 wind in the CTR and LGM simulations is stronger compared to ERA. This systematic error is

264 assumed to have only a minor impact on our results. Indeed, most of the differences turn out to be
 265 less important for the further use in this study, except larger precipitation over western China at 37°N
 266 on the northern slope of the Kunlun Shan in the C&L data set, which is investigated in more detail
 267 in Appendix S2 of Supporting Information. Also in the area 105°-110°E / 35°-40°N, the drop of
 268 precipitation during LGM may be important, as discussed below in section 6.
 269
 270

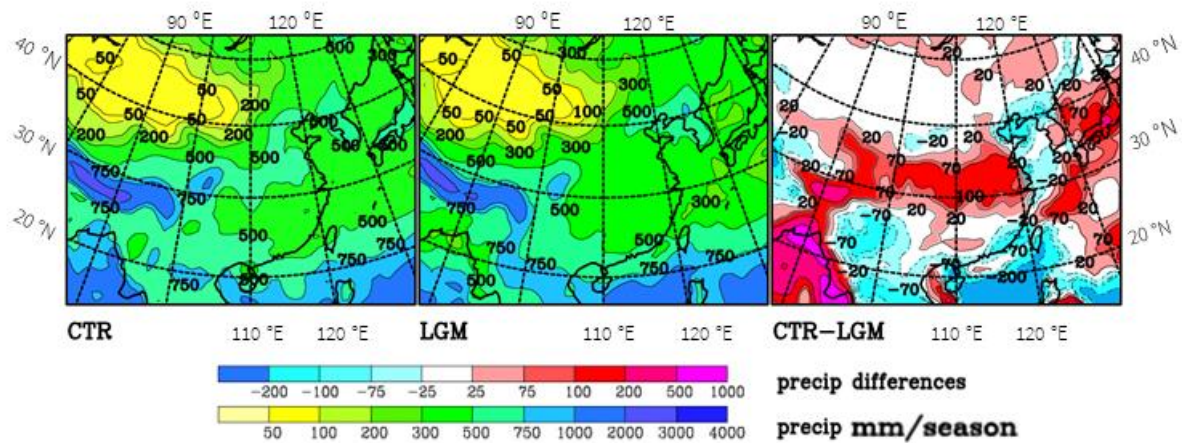


271
 272 Fig. 4: Summer (JJA) precipitation over Eastern Asia as analyzed by Leemans, R. and Cramer
 273 (1991) (C&L), ERA and GPCC and as simulated for the present (CTR). Differences between the
 274 various fields are shown. Units: mm/season

275
 276 Below we will concentrate on summer precipitation because that is the time when plants need water
 277 most. Other scientists use the annual mean precipitation as a limiting factor (e.g. Tian et al., 2016).
 278 When comparing the analyses with the model simulations for the present (CTR), one finds that the
 279 model fits better to GPCC and least to ERA (Fig. 4) away from the high mountain ranges where the

280 agreements between the different precipitation climatologies is very low. The amounts of
 281 precipitation in ERA is on a large scale higher than the other ones. For most of China south of 35°N
 282 the precipitation in ERA is much lower than in the other climatologies. The belt with stronger
 283 precipitation at 25 to 35°N in CTR is assigned in Appendix S1 of Supporting Information to an
 284 earlier northward propagation of the monsoon front in CTR compared to ERA, that is weakened
 285 from the CTR to LGM, which results in a belt of largest differences between the present and the
 286 LGM of up to 150 mm (Fig. 5). Kim et al. (2008) found similar differences in their higher resolution
 287 simulation, though spreading further north. In Appendix S1 of Supporting Information, it is shown
 288 that the monsoon, as represented by the wind direction, does not change much over the continent
 289 between the present and the LGM, and with the monsoon front propagating northward already in
 290 June the wind speeds increase. This is somewhat in contrast to results by Jiang and Lang (2010) who
 291 showed for the ensemble mean of model simulations (all with a much lower horizontal resolution
 292 than the one used here) a reduction of the JJA wind speeds. The lower JJA precipitation during LGM
 293 may also result from lower temperatures during LGM, when the atmosphere can carry only a lower
 294 amount of water vapour.

295 While Tian and Jiang (2016) found in PMIP3 simulations a general decrease of precipitation, we
 296 find it only for a belt at 29-36° N where the model shows already too large values for the present
 297 (CTR-C&L in Fig. 4).



298

299 Fig. 5: Summer (JJA) precipitation simulated for Eastern Asia and differences. Between CTR and
300 LGM. Units: mm/season.

301

302 **4 COMPARING POLLEN INFORMATION WITH CLIMATIC DATA**

303 In Leroy and Arpe (2007) and Arpe et al. (2011), climatic data were combined to find the areas
304 where temperate deciduous trees could survive due to limiting criteria and then compared that with
305 palaeo-data of such trees for Europe. The same method is now applied for Eastern Asia. Europe is
306 limited to the south by steppe and by the Mediterranean Sea. However, in E. Asia, a vast
307 subtropical area with deciduous temperate trees mixed with conifers and broadleaved evergreens
308 (i.e. between biomes TEDE and WTEM of Ni et al., 2010) lies south of the temperate deciduous
309 forest (Qiu et al., 2011). It was therefore essential to add a climatic limit to separate these two main
310 vegetation types. In addition to the limits used for Europe, we add also a maximal winter
311 temperature (T_{max}) which the climatological temperature must fall below to allow deciduous tree
312 to grow but not the evergreens tree, suggested by Sitch et al. (2003) and Roche et al. (2007) (Table
313 1). Sitch et al. (2003) require a less strong limit of $-17\text{ }^{\circ}\text{C}$ minimum temperature and $+15.5\text{ }^{\circ}\text{C}$
314 maximum temperature of coldest month for temperate deciduous trees but only for very few sites
315 such a relaxation of limits would decrease the number of sites that fail the comparison with the
316 climatological estimate. Roche et al. (2007) used for temperate broadleaf forest $T_{min}=-2\text{ }^{\circ}\text{C}$ and
317 T_{max} of $+5\text{ }^{\circ}\text{C}$. We regard a T_{min} limit of $-2\text{ }^{\circ}\text{C}$ only valid for warm-loving deciduous trees.

318

319

320

321

322

323

324

325

326 Table 1: Limiting factors for temperate deciduous tree growth used in this study.

327 Tmin = minimum temperature of the coldest month, Tmax = maximum temperature of the coldest month,

328 GDD5 = growing degree days for which the excess over 5°C is accumulated for each day,

329 JJA precipitation = accumulated summer precipitation.

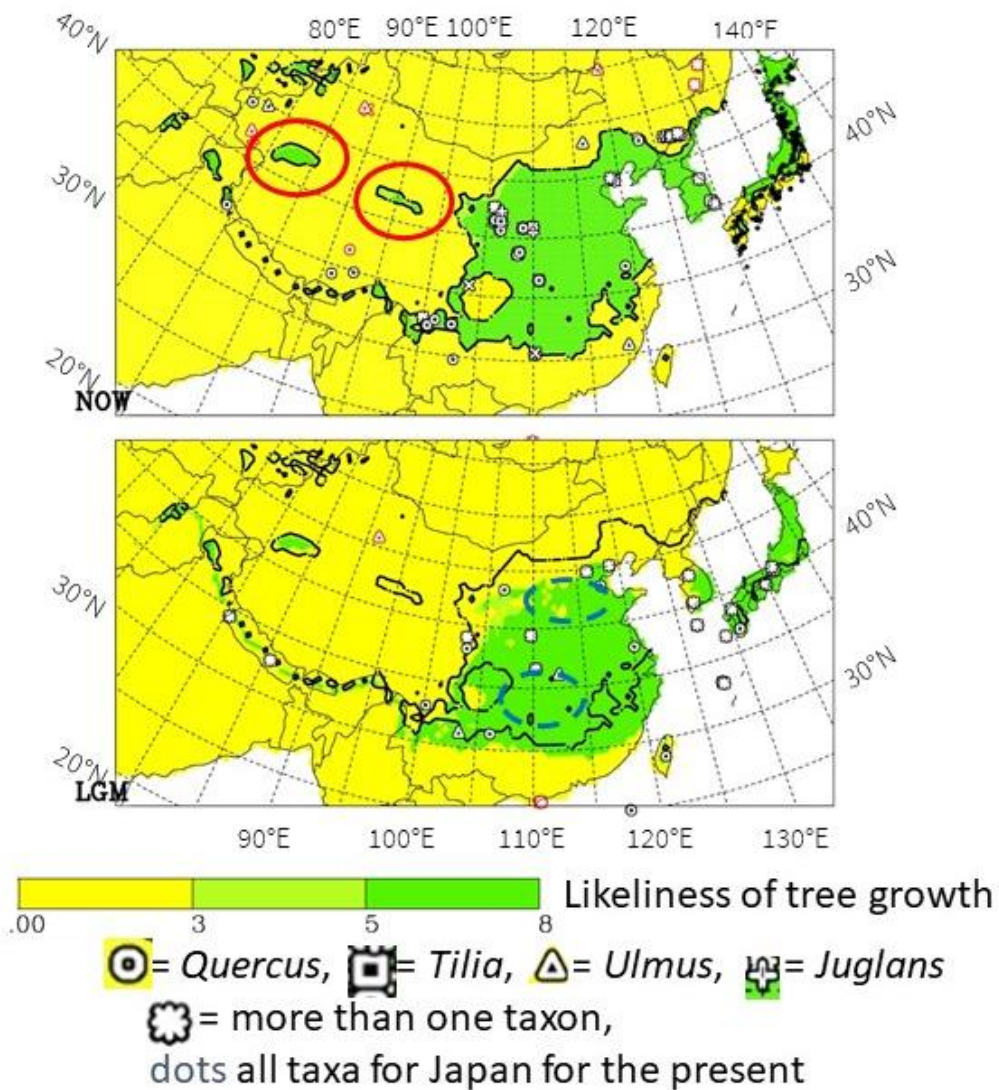
330

Tmin	Tmax in winter	GDD5	JJA precipitation
-15°C	+5°C	800	50 mm/summer

331

332

333 When combining these limits with the climate data we arrive at the distribution shown in Fig. 6.



334

335 Fig. 6: Possible tree growth according to our limitations given in Table 1. Darker colours (green)

336 mean that the climate data suggest possible tree growth. For easier comparison between the present

337 (upper panel) and the LGM (lower panel), the limits for the present are copied as a solid line into

338 the LGM panel. Markers indicate where and which tree pollen of deciduous trees are found.

339 Markers: circles = *Quercus*, squares = *Tilia*, triangles = *Ulmus*, plus = *Juglans* and stars = more

340 than one taxon. For modern-day sites in Japan only dots are used for clarity of the plot. Open

341 markers = at least within a distance of ± 3 grid points (~ 150 km radius) the climate data suggest

342 possible tree growth; otherwise filled (red) markers. Red and blue (dashed) ovals show areas of
343 interest mentioned in the text.

344

345 Only very few stations with observed pollen are outside (not within a distance of ± 3 grid points,
346 i.e. about ~150 km radius) the area of possible tree growth according to our criteria (filled markers
347 see also Tables 2 a and b for the LGM). For the present, 13 out of 380 stations with observed
348 deciduous tree pollen do not fit to the climate data of the present, most of them because of too cold
349 winter temperatures (-20 to -23 °C), one at 91°E, 31°N because of a too short summer (GDD5 <
350 600), two (both at 109 °E, 18 °N) because of too warm winter temperatures (>17 °C) and one (77
351 °E, 37 °N) because of lack of summer precipitation and too cold winter temperatures, though these
352 are both near given limits. South-eastern Japan is often too warm in winter for deciduous trees
353 though there are many observations in that area. These stations are, however, within 3 grid points
354 to areas that are marked as suitable for their growth.

355 In Fig. 6 for the present, two areas marked by red ovals in western China at latitude 37 °N indicate
356 possible tree growth according to the climatic data where the precipitation in the C&L climatology
357 (Fig. 4) exceeds the ones of ERA and GPCC considerably. Also ERA and GPCC show relative
358 maxima at 37 °N in that area but shifted by 5 ° to the east. We believe that the precipitation by
359 C&L is deficient here, as explained in Appendix S2 of Supporting Information.

360 In the southern China Sea around 120°E,28°N only one marker with observed tree pollen for the
361 LGM is shown in fig. 6 although around that position four cores are available (see Table 2 for
362 details). All four observations agree with the possibility of trees according to the climate estimate.
363 Because of the use of marine sediment, pollen must have been transported from the land, which is
364 further discussed in the next section.

365 In Eastern Asia, some species might have evolved which are hardier than those of the same genus
366 present in Europe. Fang et al. (2009) show *Ulmus pumila* over large areas of northern China and
367 SE Siberia, a species that can withstand extremely cold temperatures in winter and drought (Solla

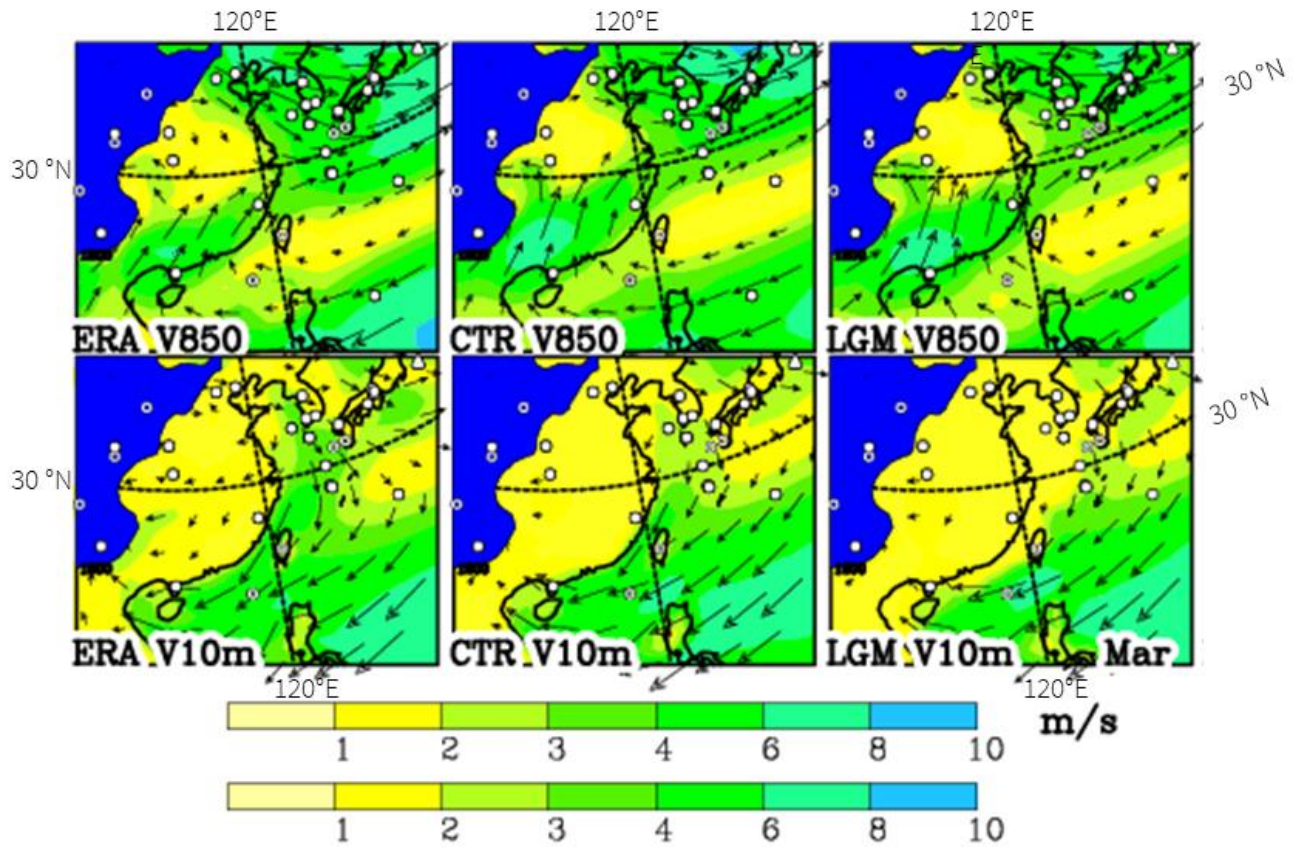
368 et al., 2005). *Ulmus* has the most failures in our comparison with model data. Fang et al. (2009)
369 show a wide spread of *Tilia amurensis* in NE China, SE Siberia and N Korea, which is also absent
370 from Europe. This tree, like the elm, is extremely frost hardy (Piggott, 2012).

371

372 **5 POSSIBLE TREE GROWTH DURING THE LGM**

373 Thirty-five pollen sites for the LGM were used (Table 2). A good overall fit occurs between the
374 climate data and the LGM pollen data. In Fig. 6 lower panel, only two filled markers, not agreeing
375 with climate data, are found on the continent. The site of Huguangyan in the south has winter
376 temperatures higher than 10° C, which are too high for deciduous trees. In the north-west China in
377 the Tarim basin is another filled marker. The observation consists of only 1% pollen for *Ulmus*.
378 There the winter temperatures are -17 °C, just outside the limit used here (Table 1) but within the
379 limits suggested by Sitch et al. (2003). On Hokaido a filled marker indicates a disagreement between
380 climate and pollen observation but it is only slightly too cold in winter (-15.7 °C).
381 Four cores in the deep ocean in the S. China Sea are marked in Table 2 and Fig. 6 as not agreeing
382 with our given limits when using the down-scaled climate data, but because of the deep sea the pollen
383 must have been transported there. From Fig. 7, it can be concluded that the pollen could only have
384 come with the north-easterly 10m wind from Taiwan where also *Quercus* was found during the LGM
385 (Table 2). As the present blooming period for *Quercus variabilis*, a widespread species of the
386 deciduous forest, is January to March in Taiwan (Liao, 1996), the winds during March are shown in
387 Fig. 7, assuming a little later blooming period during the cooler LGM than presently, though the
388 wind fields for March and February are hardly different. When taking the wind at a higher level (850
389 hPa or around 1500m), the wind is blowing more from the east in accordance with the Ekman spiral
390 in the atmospheric boundary layer. Therefore, pollen must have travelled near the surface when
391 coming from Taiwan or if it arrived at higher levels it may have come from the Philippines (Luzon)
392 that however seems to be too far south for deciduous oak and, moreover, this area is not suggested
393 in our estimate of having possible deciduous tree growth (Fig. 6).

394 Thus, the area boundaries for the present and for the LGM are only slightly different with a shift
 395 for the LGM by 2 to 3° to the south of both the northern and southern limits, and an eastwards shift
 396 of the western boundary. In northern China, Korea and north Japan (Hokkaido), differences result
 397 mainly from the winter minimum temperatures, as can be seen from Fig. 1 in which winter
 398 temperatures drop by more than 6°C from the present to the LGM.



399
 400 Fig. 7: Winds at 10m (V10m) and at 850hPa (V850) for March as analysed (ERA) and simulated
 401 for the present (CTR) and LGM. All panels are showing the prevailing north easterlies. Areas with
 402 topography above the 850hPa level are erased and blue coloured. Observational sites for the LGM
 403 are indicated by markers
 404
 405

406 Table 2: Selected sites with observed pollen during the LGM. "*Quercus*" include deciduous
 407 *Quercus* and *Lepidobalanus*, "*Ulmus*" includes *Ulmus-Zelkova*, and "others" include: *Carya*, *Tilia*,
 408 *Carpinus*.

409 "Agree" means that the observations agree with our estimates of possible tree growth as shown in
 410 Fig. 6 or 8 respectively.

411

412 Table 2a: east of 120°E

Lon E	Lat N	Site	Region	Alt/ depth in m	<i>Quercus</i>	<i>Ulmus</i>	Other	Agree	Author
126°32'	33°14'	HN-1, Hanon maar	Jeju Island	53			Y	Y	4
126°33'	33°15'	BH-4B	Jeju Island	53	Y	Y	Y	Y	5
126°52'	35°12'	Yeonjaedong Trench	Gwangju	20?	Y	Y		Y	6
127°13'	33°15'	UD-2	Hanam	19	Y	Y		Y	7
128°04'	35°10'	Pyonggeodong	Jinju	30			Y	Y	8
128°57'	38°33'	MD982195	N of E. China Sea	-746	Y			Y	9
130°23'	31°49'	Imutaike Pond	Southern Kyushu	330	Y			Y	10
130°23'	33°36'	Tenjin	Tenjin Fukuoka city, N Kyushu	0		Y	Y	Y	11
134°36'	34°24'	Ohnuma	Chugoku Mts	610	Y		Y	Y	12
135°48'	35°12'	Hatchodaira	Kyoto	810	Y	Y	Y	Y	13
135°53'	35°32'	Iwaya	Fukui	20		Y	Y	Y	14
135°53'	35°33'	Lake Mikata	C Japan	0		Y	Y	Y	15
138°53'	36°49'	Lake Nojiri	C Japan	250	Y	Y	Y	Y	16
140°10'	36°03'	Hanamuro River HS1	C Japan	5	Y	Y	Y	Y	17
139°40'	36°41'	Nakazato	C Japan	183	Y	Y	Y	Y	18
141°47'	36°04'	MD01-2421	off Kashima	-2224	Y	Y	Y	Y	21c
130° 42'	35°56'	KCES-1	Sea of Japan	-1464	Y	Y		Y	19
142 12.08	41 10.64	C9001C	NE Japan	-1180	Y	Y	Y	?	20
136°03'	35°15'	BIW 95-4	Lake Biwa	85	Y	Y		Y	21a
142°28'	44°03'	Kenbuchi	Hokaido	137	Y	Y	Y	N	21b

413

414 Authors: 4: Park and Park 2015; 5: Chung 2007; 6: Chung et al. 2010; 7: Yi and Kim 2010; 8: Chung et al. 2006; 9: Kawahata and
 415 Ohshima 2004; 10: Shimada et al. 2014; 11: Kuroda and Ota, 1978; 12: Miyoshi and Yano, 1986; 13: Takahara and Takeoka, 1986; 14:
 416 Takahara and Takeoka, 1992; 15: Nakagawa et al. 2002; 16: Kumon et al. 2003; 17: Momohara et al. 2016; 18: Nishiuchi et al. 2017;
 417 19: Chen et al. 2016; 20: Sugaya et al. 2016; 21a: Hayashi et al. 2010; 21b: Igarachi and Zarov 2011; 21c: Igarachi 2009

418 Table 2b: west of 120°E

Lon E	Lat N	Site	Region	Alt/ depth in m	<i>Quercus</i>	<i>Ulmus</i>	Other	Agree	Author
80°08'	29°20'	Phulara palaeolake	Kumaun Himalaya	1500?	Y	Y	Y	Y	1
85°18'	27°14'	JW-3	Kathmandu valley	1300	Y		Y	Y	2
93°49'	27°32'	Ziro valley	Arunachal Pradesh	1570	Y		Y	Y	3
91°03'	40°47'	CK2	Tarim basin	780	Y			N	22
99°57'	27°55'	06SD, lake Shudu	Yunnan	3630	Y			N	23
102°47'	24°20'	XY08A, Xingyun Lake	C Yunnan	1772	Y		Y	Y	24
102°57'	33°57'	RM Ruergai	Zoige basin	3400	Y	Y		Y	26
103°30'	32°55'	Wasong	NE Tibetan Plateau	3490	Y			Y	27
106°30'	38°17'	Shuidonggou locality 2	Yinchuan, Ningxia	1200	Y	Y		Y	28
109°30'	34°24'	Weinan	Loess Plateau	650	Y	Y	Y	Y	29
110°00'	31°29'	DJH1, Dajiuhu	Shennongjia Mountains	1751	Y	Y	Y	Y	30
110°17'	21°09'	Huguangyan maar	southern China	23	Y	Y	Y	Y	31
115°57'	39°45'	East part	Yan Shan	150?	Y	Y	Y	Y	32
117°23'	20°07'	17940	S China Sea	-1727	Y			N	33
117°25'	20°03'	ODP 1144	S China Sea	-2037	Y			N	34
117°21'	20°08'	MD05-2906	S China Sea	-1636	Y	Y	Y	N	35
119°02'	26°46'	SZY peat bog	Fujian	1007	Y			Y	36
120°53'	23°49'	Toushe Basin	Taiwan	650	Y		Y	Y	37
127°16'	28°09'	DG9603	China Sea	-1100	Y			Y	38
127°22'	28°07'	MD982194	Okinawa Trough	-989	Y	Y		Y	39
118°16'	20°20'	STD235	S China Sea	-2630	Y	Y	Y	N	40

419

420 Authors: 1: Kotlia et al. 2010; 2: Fuji and Sakai 2002; 3: Bhattacharyya et al., 2014; 22: Yang et al., 2013; 23: Cook et al. 2011; 24:

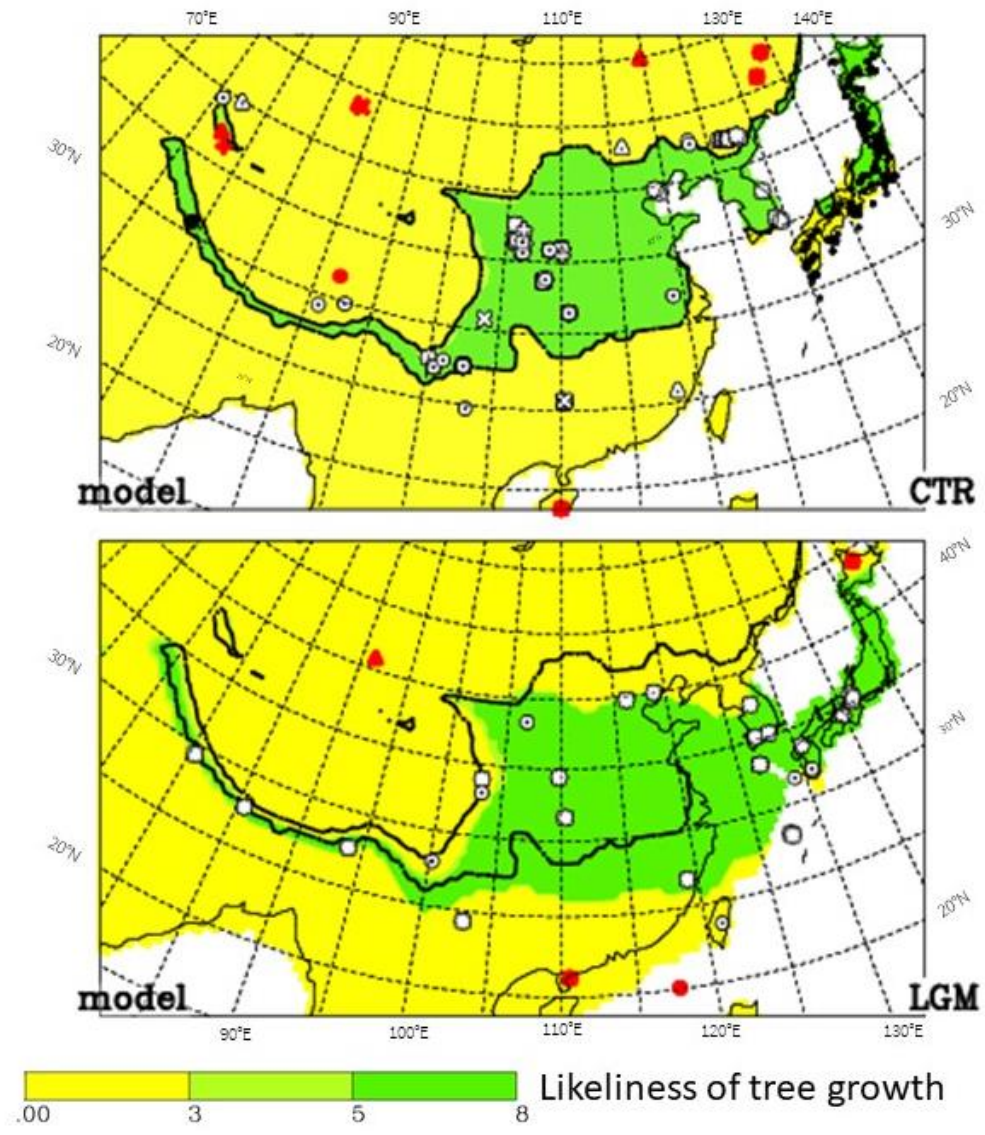
421 Chen et al. 2014 and Chen XM et al. 2015 IPS abstract; 26: Shen et al. 2005; 27: Yan et al. 1999; 28: Liu et al. 2011; 29: Sun et al.

422 1996; 30: Li et al. 2013; 31: Wang et al., 2012, Lu et al., 2003; 32: Xu et al. 2002; 33: Sun & Li 1999; Sun et al. 2000; 34: Sun et al.

423 2003; 35: Dai et al. 2015; 36: Yue et al. 2012; 37: Liew et al. 2006;

424 38: Xu et al. 2010; 39: Zheng et al. 2013; 40: Yu et al. 2017.

425 The down-scaling method used here does not allow us to present values over the emerged shelf of
426 the Yellow Sea during the LGM, when the mean sea level was 120 m below the present one
427 (Lambeck et al., 2014). Therefore, in Fig. 8, the possible tree distribution is shown using model
428 data without down-scaling, when the high spatial resolution is lost and more impacts from
429 systematic errors of the model may be expected. However, fortunately, such impacts can hardly be
430 seen when comparing Fig. 6 with Fig. 8, except for the present along the southern slopes of the
431 Himalayas and the southern border of possible tree growth, where T2m by C&L is lower than that
432 of CTR (also than that by ERA), leading to a better fit with pollen data when using T2m by C&L.
433



434

435 Fig. 8: same as Fig. 6 using model data without down-scaling. The Yellow Sea is shown as land in
 436 the LGM.

437

438 **6 LGM CONNECTIVITY AND DISTRIBUTION MAPPING**

439 The results show two worth-discussing areas with population connectivity: one is over the Yellow
 440 Sea emerged shelf and one along the south of the Himalayan Range.

441 The northern limit of the temperate deciduous trees assumed by previous research (Harrison et al.,
442 2001, their figure 1) is much further south (30 - 35 °N) than what is found here. Therefore,
443 population connectivity over the shelf was rejected by Harrison et al. (2001). It should be
444 mentioned that the results by Harrison et al. (2001) were based on the model available at that time
445 which had a lower resolution and also was based on observational data available at that time,
446 which have improved considerably since then. Indeed 80% of the sites used in the current
447 investigation were published post-2001. Moreover, the Harrison et al. (2001) study is based on
448 biomes, not tree occurrences. Three arguments can be presented now to support this connectivity.

449 Firstly, the model results clearly show the connectivity of tree populations between China, Korea
450 and Japan during the LGM over the emerged shelf. This connectivity takes place because the limit
451 of the possible tree growth of our investigation (darker areas in Fig. 8 as well as in Fig. 6) reaches
452 still quite far north (40 °N), which is in accordance with pollen data.

453 A second argument is the presence of deciduous trees in sites located around the shelf in amounts
454 suggesting larger than simple tree presence, even perhaps woodlands or forests. In several places
455 around the emerged shelf the percentages of temperate deciduous trees indeed exceed 10%, e.g. in
456 the Yeonjaedong swamp in Korea with 20-30% of deciduous *Quercus*, 7-20 % of *Ulmus-Zelkova*
457 (Chung et al., 2010), the two sites on the Jeju island maar lake (Chung, 2007; Park and Park,
458 2015), Tenjin peatland in Japan with 12% deciduous *Quercus*, 8% *Carpinus*, 2.5% *Tilia* (Kuroda
459 and Ota, 1978), and the marine cores DG9603 and MD982194 with 15% of deciduous *Quercus*
460 (Xu et al., 2010).

461 Thirdly, information derived from recent phylogenetic investigations is supportive of the
462 occurrence of deciduous trees on the emerged shelf. For example, the phylogeography of one of
463 the most widely distributed deciduous species in eastern Asia, the oak, *Quercus variabilis*, clearly
464 suggests the occurrence of land bridges over the East China Sea (Chen et al., 2012). Around the E.
465 China Sea, other phylogenetic data indicate both mixing and absence of mixing between
466 populations depending on plant type (Qi et al., 2014). The occurrence of mixing indicates that

467 contacts were possible across the emerged shelf (e.g. Tian et al., 2016); while the absence of
468 mixing for other species indicate that not all species mixed, but certainly does not suggest total
469 absence of migration for other species. It appears therefore that the E. China Sea acted as a filter,
470 letting some through, others not (Qi et al., 2014).

471 The eastern Asian case is very different from Europe, where fragmentation is the rule in the LGM.
472 In Europe (Fig. 2), the temperatures were much lower than presently (8 to 15 °C) compared to
473 Eastern Asia (3 to 5 °C) and therefore the shift of possible temperate deciduous tree growth is
474 much smaller in E. Asia than in Europe. Phylogenetic results in E. Asia are indeed in favour of the
475 hypothesis of species surviving both in the north and the south of China (Qian and Ricklefs, 2000)
476 and not of species surviving only in the south (Harrison et al., 2001). The basic expansion-
477 contraction model of vegetation belts in Europe was much less important in Eastern Asia (Qiu et
478 al., 2011), due to the smaller Asian ice cap and a different topography (López-Pujol et al.,
479 2011) . Eastern Asia biodiversity was therefore preserved across the Ice Ages, owing to not only
480 the more moderate lowering of temperatures but also to the better connectivity between
481 populations

482 One question, was if the pollen, found in the emerged shelf of the Yellow Sea is produced locally
483 or remotely. According to the Harrison et al. (2001) study, these pollen grains must have come
484 from the southern part of China. Yu et al. (2004) have tried to calculate such long-distance
485 transports. For *Quercus* and *Ulmus* they found transports of up to 6 ° latitude/longitude in any
486 direction. This would be too short for a transport from China south of 30 °S. Also the high pollen
487 percentages at the observed sites speak against such a long-distance transport.

488 We are not convinced that Yu et al. (2004) calculations are robust enough for using their results in
489 our investigation, especially as their figure 3 does not agree with plant distributions by Fang et al.
490 (2009). Therefore, the wind fields for the present as analysed by ECMWF (ERA) and as simulated
491 by our model for the LGM were investigated. In Appendix S1 of Supporting Information as well as
492 in Fig. 7, it is shown that ERA and the simulation for the present agree quite well, at least for the

493 wind directions, which makes us confident that we can use the model simulations for the LGM
494 straight away.

495 The winds at 10m and 850 hPa for March, a central month for the blooming of *Quercus variabilis*,
496 are shown in Fig. 7 for the present (ERA), the CTR and the LGM. Over the emerged shelf of the
497 Yellow Sea, the 10m winds are very light from the north-west during the LGM (much stronger in
498 ERA because of the lower surface friction over the sea). For the higher level of 850 hPa, all data
499 sets show very similar distributions all with north-westerlies. Long-distance transport of deciduous
500 tree pollen would have come from NE China, an area that Harrison et al. (2001) assume to be void
501 of deciduous trees, though some recent studies (including the present one) indicate the opposite
502 (Yu et al., 2004). Further on in the year, the 850 hPa winds are blowing from the south-west,
503 starting in April and fully crossing the 30 °N latitude in May (similar to CTR in Fig. S1.1), i.e. a
504 transport from mainland China would have been possible, though a little late for the main
505 blooming of the deciduous oak. In Appendix S1 of Supporting Information, it is shown for the
506 present that the simulations suffer from a too early progression of the monsoon front, which
507 suggests that the turn of the wind to south-westerlies may have occurred also later for the LGM,
508 thus leading to a less likely transport from mainland China.

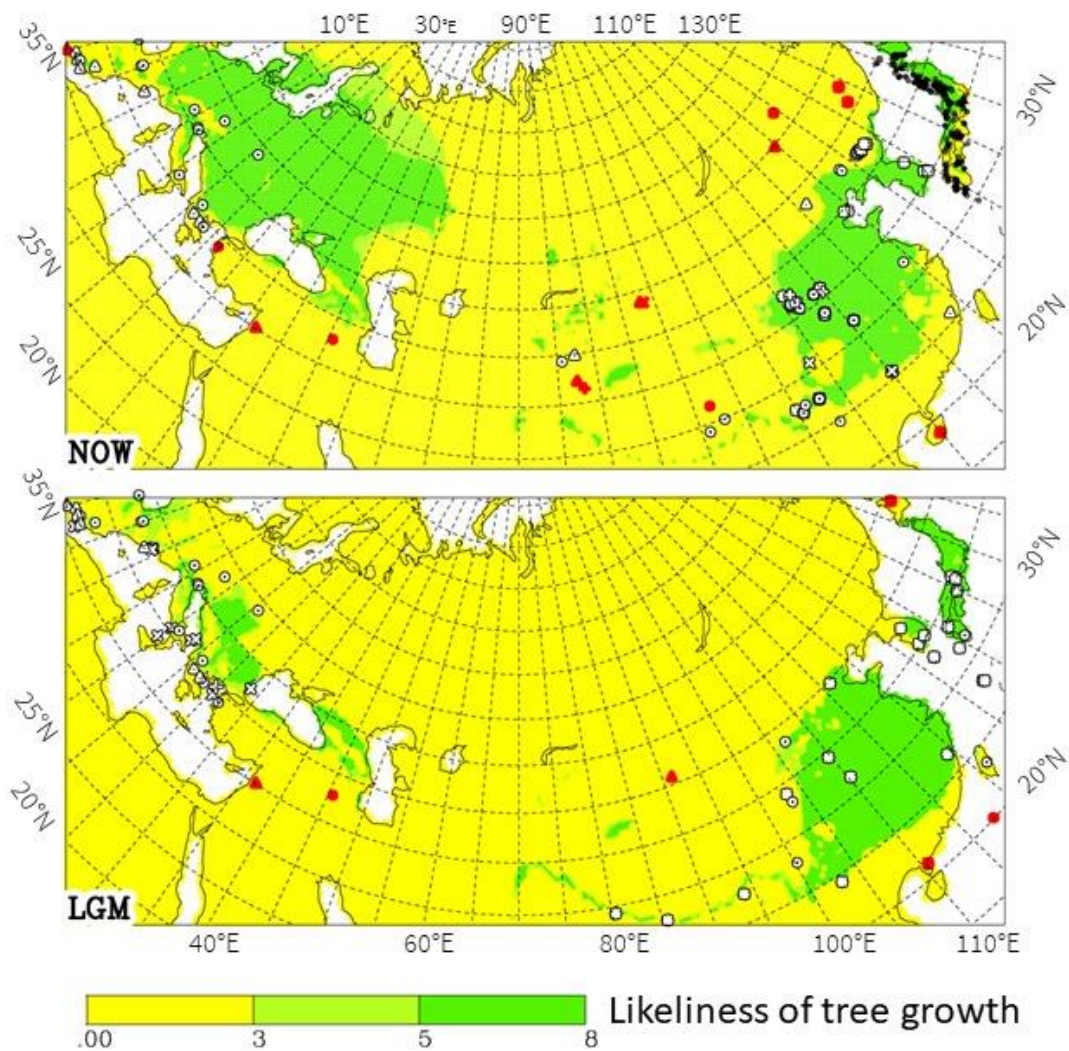
509 The source for the pollen found in the emerged Yellow Sea is not completely clear but May is late
510 for the blooming season in central China (for Taiwan it is January to March). Therefore, a local
511 production or transport from northern China is more likely, supporting our argument that the
512 emerged Yellow Sea was occupied by deciduous trees during the LGM, as indicated by Fig. 8.
513 Another important population connectivity result is that the Himalayas were more favourable to
514 temperate deciduous trees in the LGM and provided the possibility of a quasi-continuous band of
515 temperate forest at its southern slope, beneficial for the spreading and diffusion of genes (e.g. for
516 Chinese mole shrew, He et al., 2016), more so than in the present (Fig. 6). Three observational
517 sites, that are currently available, support this chain of possible tree growth during the LGM. For
518 the present, this link does not exist because of too warm winter temperatures (warmer than 5 °C in

519 the C&L climatology). Along the slopes of the high Himalayas it is most likely that there would be
520 a level at which the temperature will be below 5 °C (an issue which needs further investigation).

521 Two significant cases occur where population connectivity was higher, indicating less population
522 fragmentation, in glacial than in interglacial periods. So, it appears that many tree populations live
523 nowadays in interglacial refugia.

524 During LGM the precipitation and the temperature were lower than at the present. Which of both
525 was more important for the tree growth cannot be said with certainty. Tian et al. (2016) stated:
526 “annual precipitation is considered as the most important determinant”, and in our study we have
527 some indication to agree with that. In Fig. 6 and 8, there is a cluster of pollen findings over central
528 China (105-110°E/35-40°N) for the present but not for LGM. In this area the temperature does not
529 change much (Fig. 2 and 3) but the summer precipitation decreases substantially (Fig. 5). This
530 change is only slightly reflected by the boundaries of possible tree growth in Fig. 6 (north of 40°N.
531 The lack of observational sites with pollen of tree pollen is not a proof, because it could be due to
532 many reasons, but the massive change in occurrence is suggestive that we should have perhaps
533 increased summer precipitation requirements for tree growth (Table 1). This can, however, also
534 indicate the reduced water use efficiency of the trees at LGM due to lower atmospheric CO₂.
535 Finally, this investigation shows that the model simulations suggest possible tree growth where
536 pollen grains of such trees are found. This leads to the possibility of using the model data to fill
537 gaps between observational sites by way of maps. Such gaps especially occur around 30-37 °N /
538 105-120 °E and 25-30 °N / 110-115 °E, i.e. the provinces Hupeh to Kiangsu and Hunan (ovals in
539 Fig. 6 lower panel).

540



541

542 Fig. 9: same as Fig. 6 for the whole of Eurasia. Pollen data for Europe have been described by
 543 Arpe et al. (2011). Darker colours (green) are areas in which trees are able to grow according to
 544 model data. Lighter green are areas where not all criteria are completely fulfilled

545 By extending the view of our investigation for the whole of Eurasia (Fig. 9), a stronger link
 546 between China and Europe is shown during the LGM than presently. Along the foot of the
 547 Himalayas, a continuum existed; but westwards of it, still a gap north of Afghanistan (probably
 548 going back to the Tertiary) is maintained, inhibiting a total link across Eurasia. This continuum is
 549 broken for the present climate by model results because winter temperatures exceed 7 °C, hence
 550 being too warm for temperate deciduous trees.

551 **7 CONCLUSIONS**

552 Generally, the estimates of possible temperate deciduous tree growth in the LGM in eastern Asia
553 by model simulation agree with fossil pollen observations. Therefore, the model estimates can fill
554 the areas without observations. The results in the form of LGM distribution maps are considered
555 robust enough as model simulations for the present are within the range of climate estimates.
556 Nevertheless, we are aware of some uncertainties in the climate of Eastern Asia and we can safely
557 say they are not a limitation of this study.

558 During the LGM, major connectivities between populations are found, which is in agreement with
559 observation, i.e. less tree population fragmentation. This is especially visible in two places. Firstly,
560 the link between China, Korea and Japan is clear. Sufficient new pollen studies around and on the
561 emerged Yellow Sea shelf are now available, confirming the results of the model. They suggest the
562 presence of temperate deciduous trees, perhaps even woodlands, in the area.

563 Secondly, connectivity during the glacial period occurred at the southern slope of the Himalayan
564 chain favouring genetic flow in interglacial refugia. Currently this link does not exist because of
565 too warm winter temperatures there. Our simulations cannot be taken as a proof of this hypothesis,
566 as one cannot imagine that along the Himalayan chain there would not be a level at which the
567 winter temperatures do not exceed 5 °C also for the present day, a higher resolution data set would
568 be able to show how wide and continuous such a corridor of possible tree growth would be at the
569 present.

570

571 Another outcome of this research is the contribution to the conservation agenda (López-Pujol et al.,
572 2001). The areas of LGM refugia often match areas of present hotspots of biodiversity. Hence the
573 distribution of temperate forest obtained in our investigation can serve as a guide to establish
574 nature parks for plants and animals. Moreover the difference between LGM and present
575 distribution contribute to the understanding of rate of distribution change (as well genetic flow),
576 which is important to monitor in light of possible climatic change.

577

578 **ACKNOWLEDGMENTS**

579 Jing Zheng (Fujian Agriculture and Forestry University) started collecting the LGM data during a
580 post-doctoral stay with Suzanne Leroy at Brunel University London. Uwe Mikolajewicz
581 acknowledges funding from the German Federal Ministry of Education and Research in its
582 research framework for sustainable development (FONA3, FKZ 01LP1502A).

583

584

585 **AUTHORS CONTRIBUTION**

586 S.A.G. Leroy

587 Looking after conceptual issues, collecting the data, writing the manuscript

588

589 K. Arpe

590 Writing most of the manuscript, preparing the figures and responsible for meteorological
591 and climatological issues

592

593 U. Mikolajewicz

594 Providing the model simulations

595

596 J. Wu

597 providing observational tree pollen data

598

599

600 **The authors declare that they have no conflict of interest**

601 **Code availability**

602 The model version is already widely known and available. We have clearly described what has
603 been done and the follow up programs are written in FORTRAN This can be requested from Klaus
604 Arpe if wanted

605 **Data availability**

606 Table 2 provides a list of all observational sites and observational tree pollen data. Most of the
607 other data are referred to by giving the website .It does not seem feasible to provide the model
608 simulation data in a simple way. They can be obtained from Klaus Arpe in GRIB format.

609
610

611

612

613

614

615 **REFERENCES**

616 Annan, J. D. and Hargreaves J. C.: A new global reconstruction of temperature changes at the Last
617 Glacial Maximum. *Clim. Past*, **9**, 367–376, 2013.

618

619 Arpe K., Leroy S.A.G. and Mikolajewicz U.: A comparison of climate simulations for the last
620 glacial maximum with three different versions of the ECHAM model and implications for
621 summer-green tree refugia. *Clim. Past*, **7**, 1–24, 2011.

622

623 Becker A, Finger P, Meyer-Christoffer A, Rudolf B, Schamm K, Schneider U, Ziese M : A
624 description of the global land-surface precipitation data products of the Global Precipitation
625 Climatology Centre with sample applications including centennial (trend) analysis from 1901
626 present. *Earth Syst. Sci. Data* 5: 71-99, DOI: 10.5194/essd-5-71-2013, 2013.

627

628 Bhattacharyya A., Mehrotra N., Shah S. K., Basavaiah N., Chaudhary V., Singh IB, and Singh I.B.:
629 Analysis of vegetation and climate change during Late Pleistocene from Ziro Valley, Arunachal
630 Pradesh, Eastern Himalaya region. *Quatern Sci Rev* 101, 111-123, 2014.

631

632 Braconnot P., B. Otto-Bliesner, Harrison S., Joussaume S., Peterchmitt J-Y. Abe-Ouchi M.,
633 Crucifix M., Driesschaert E, Fichetfet Th., Hewitt C. D., Kageyama M., Kitoh A., **Lainé A.**,

634 Loutre M.-F., Marti O., Merkel U., Ramstein G., Valdes P., Weber S. L., Yu Y., and Zhao Y. :
635 Results of PMIP2 coupled simulations of the Mid-Holocene and Last Glacial Maximum – Part
636 1: experiments and large-scale features. *Clim. Past*, 3, 261–277, 2007.
637

638 Cao, X., Ni, J., Herzsuh, U., Wang, Y. and Zhao Y.: A late Quaternary pollen dataset from
639 eastern continental Asia for vegetation and climate reconstructions: Set up and evaluation.
640 *Palaeobot Palyno* 194, 21–37, 2013.
641

642 Chen D., Zhang X., Kang H., Sun X., Yin S., Du H., Yamanaka N., Gapare W., Wu H. X. and Li
643 C. : Phylogeography of *Quercus variabilis* Based on Chloroplast DNA Sequence in East Asia:
644 Multiple Glacial Refugia and Mainland-Migrated Island Populations. *PloS One*, 7,10: e47268.
645 doi:10.1371/journal.pone.0047268, 2012.
646

647 Chen W.-Y., Su T., Adams J.M., Jacques F.M.B., Ferguson D.K. and Zhou Z.-K: Large-scale
648 dataset from China gives new insights into leaf margin–temperature relationships. *Palaeogeogr*,
649 *Palaeocl* 402, 73–80, 2014.
650

651 Chen J., Liu Y., Shi X., Bong-Chool S., Zou J. and Yao Z.: Climate and environmental changes for
652 the past 44 ka clarified in the Ulleung Basin, East Sea (Japan Sea). *Quat Int*, 1-12, 2016,
653

654 Chen X.M., Chen F., Zhou A., Wu D., Chen J. and Huang X.: Vegetation history, climatic changes
655 and Indian summer monsoon evolution during the last 36400 years documented from sediments
656 of Xingyun Lake, south-west China. 13th International Paleolimnological Symposium,
657 Lanzhou, China, volume of abstracts, pages 162-163, 2015.
658

659 Chung C.-H, Lim HS and Yoon HI: Vegetation and climate changes during the Late Pleistocene to
660 Holocene inferred from pollen record in Jinju area, South Korea. Geosci J 10, 4, 423 – 431,
661 2006.

662

663 Chung C.-H. : Vegetation response to climate change on Jeju Island, South Korea, during the last
664 deglaciation based on pollen record. Geosci J 11, 2, 147 – 155, 2007.

665 Chung C.-H., Lim H. S. and Lee H. J.: Vegetation and climate history during the late Pleistocene
666 and early Holocene inferred from pollen record in Gwangju area, South Korea. Quatern Int 227,
667 61-67, 2010.

668

669 CLIMAP: Seasonal reconstructions of the Earth's surface at the last glacial maximum, Geological
670 Society of America, Map Chart Ser., MC-36, 1981.

671

672 Cook C. G., Jones R. T., Langdon P. G., Leng M.G. and Zhang E: New insights on Late
673 Quaternary Asian palaeomonsoon variability and the timing of the Last Glacial Maximum in
674 southwestern China. Quatern Sci Rev 30, 808-820, 2011

675

676 Cramer W. : www.pik-potsdam.de/~cramer/climate.html, last accessed 2007, 1996.

677

678 CRU: www.cru.uea.ac.uk/cru/data/hrg last accessed January 2016.

679

680 Dai L., Weng C. and Limi M: Patterns of vegetation and climate change in the South China Sea
681 during the last glaciation inferred from marine palynological records. Paleogeography,
682 Paleoclimatology, Paleoecology, 440, 249-258, 2015.

683

684 Dee D. P., Uppala S. M., Simmons A. J., Berrisford P., Poli P., Kobayashi S., Andrae U.,
685 Balmaseda M. A., Balsamo G., Bauer P., Bechtold P., Beljaars A. C. M., van de Berg L., Bidlot
686 J., Bormann N., Delsol C., Dragani R., Fuentes M., Geer A. J., Haimberger L., Healy S. B.,
687 Hersbach H., Hólm E.V., Isaksen L., Kållberg P., Köhler M., Matricardi M., McNally A. P.,
688 Monge-Sanz B. M., Morcrette J.-J., Park B.-K., Peubey C., de Rosnay P., Tavolato C., Thépaut
689 J.-N. and Vitart F: The ERA -Interim reanalysis: configuration and performance of the data
690 assimilation system. *Q J. Ro Meteor Soc* 137(656): 553–597, Part A. doi: 10.1002/qj.828, 2011.
691
692 Donoghue M. J. and Smith S. A.: Patterns in the assembly of temperate forests around the Northern
693 Hemisphere. *Phil. Trans. R. Soc. Lond. B* 359, 1633–1644, 2004.
694
695 ECMWF: http://data-portal.ecmwf.int/data/d/interim_daily/. Last accessed May 2014. Present
696 address: <https://apps.ecmwf.int/datasets/data/interim-full-mnth/levtype=sfc/>
697
698 Fang J, Wang Z and Tang Z: Atlas of woody plants in China. Higher Education Press, Beijing, pp
699 2020, 2009
700
701 Fuji R. and Sakai H. : Paleoclimatic changes during the last 2.5 myr recorded in the Kathmandu
702 Basin, central Nepal Himalayas. *J of Asian Earth Sci* 20: 255-266, 2002.
703
704 Gotanda K., Nakagawa T., Tarasov P., Kitagawa J., Inoue Y. and Yasuda Y.: Biome classification
705 from Japanese pollen data: application to modern-day and Late Quaternary samples. *Quatern*
706 *Sci Rev* 21, 647–657, 2002.
707
708 Gotanda K. and Yasuda Y. :Spatial biome changes in southwestern Japan since the Last Glacial
709 Maximum. *Quatern Int* 184, 84–93, 2008.
710

711 GPCC: ftp://ftp-anon.dwd.de/pub/data/gpcc/html/download_gate.html. Last accessed January 2014,
712 2013.

713

714 Harrison S. P., Yu G., Takahara H. and Prentice I. C. : Diversity of temperate plants in east Asia.
715 *Nature* 413, 129-130, 2001.

716

717 Hayashi R., Takahara H., Hayashida A. and Takemura K.: Millennial-scale vegetation changes
718 during the last 40,000 yr based on a pollen record from Lake Biwa, Japan. *Quaternary Res.* 74,
719 91-99, 2010.

720

721 He K., Hu N.-Q., Chen X., Li J.-T. and Jiang X.-L. : Interglacial refugia preserved high genetic
722 diversity of the Chinese mole shrew in the mountains of southwest China. *Heredity* 116: 23-32.
723 2016.

724 Igarachi Y.: Pollen record in core MD01-2421 off Kashima, North Pacific: correlation with the
725 terrestrial pollen record since MIS 6. *Jour. Geol. Soc. Japan*, 115,7, 357-366, 2009.

726 Igarachi Y. and Zharov A. E.: Climate and vegetation change during the late Pleistocene and early
727 Holocene in Sakhalin and Hokkaido, northeast Asia. *Quatern Int* 237, 24-31, 2011.

728

729 Jiang D. and Lang X.: Last Glacial Maximum East Asian Monsoon: Results of PMIP Simulations.
730 *Jour. of Clim*, 23, 5030 - 5038. DOI: 10.1175/2010JCLI3526.1, 2010.

731

732 Kawahata H. and Ohshima H: Vegetation and environmental record in the northern East China Sea
733 during the late Pleistocene. *Global Plane Change* 41,251–273, 2004.

734

735 Kim S.-J., Crowley T. J., Erickson D. J., Govindasamy B., Duffy P. B. and Lee B. Y.: High-
736 resolution climate simulation of the last glacial maximum. *Clim Dyn* 31:1–16 DOI
737 10.1007/s00382-007-0332-z, 2008.

738

739 Kotlia B. S., Sanwal J., Phartiyal B., Joshi L., Trivedi A. and Sharma C.: Late Quaternary climatic
740 changes in the eastern Kumaun Himalaya, India, as deduced from multi-proxy studies. *Quatern*
741 *Int* 213, 44–55, 2010.

742

743 Kucera, M., Weinelt, M., Kiefer, T., Pflaumann, U., Hayes, A., Chen, M. T., Mix, A. C., Barrows,
744 T. T., Cortijo, E., Duprat, J., Juggins, S., and Waelbroeck, C.: Reconstruction of Sea-Surface
745 Temperatures from Assemblages of Planktonic Foraminifera: Multi-Technique Approach Based
746 on Geographically Constrained Calibration Data Sets and Its Application to Glacial Atlantic and
747 Pacific Oceans, *Quaternary Sci. Rev.*, 24, 951–998, 2005.

748

749 Kumon F, Kawai S. and Inouchi Y.: Climate Changes between 25000 and 6000 yrs BP Deduced
750 from TOC, TN, and Fossil Pollen Analyses of a Sediment Core from Lake Nojiri, Central
751 Japan. *The Quaternary Res* 42, 1: 13-26, 2003.

752

753 Kuroda T. and Ota T.: Palynological study of the late Pleistocene and Holocene deposits of the
754 Tenjin area, Fukuoka City, northern Kyushu, part 1. *The Quaternary Res* 17, 1, 1-14. (In
755 Japanese with English summary), 1978.

756

757 Lambeck K., Rouby H., Purcell A., Sun Y., and Sambridge M.: Sea level and global ice volumes
758 from the Last Glacial Maximum to the Holocene. *PNAS* 111, 43, 15296–15303, 2014.

759

760 Leemans R. and Cramer W.: The IIASA database for mean monthly values of temperature,
761 precipitation and cloudiness of a global terrestrial grid, International Institute (IIASA). RR-91-
762 18, 1991.

763

764 Leroy S. A. G.: Progress in palynology of the Gelasian-Calabrian Stages in Europe: ten messages,
765 Revue de Micropaléontologie, 50, 293–308, 2007.
766

767 Leroy S. and Arpe K.: Glacial refugia for summer-green trees in Europe and S-W Asia as proposed
768 by ECHAM3 time slice atmospheric model simulations. J Biogeogr, 34, 2115-2128. doi:
769 10.1111/j.1365-2699.2007.01754x, 2007.

770 Li J. and Del Tredici P.: The Chinese *Parrotia*: A Sibling Species of the Persian *Parrotia*. *Arnoldia*
771 66,1: 2-9, 2008.
772

773 Li J., Zheng Z., Huang K., Yang S., Chase B., Valsecchi V., Carré M. and Cheddadi R.: Vegetation
774 changes during the past 40,000 years in Central China from a long fossil record. *Quatern Int*
775 310, 221-226, 2013.
776 .

777 Liao J. C.: Fagaceae. In *Flora of Taiwan*. Volume 2. 2nd edition. Edited by: Boufford D. E., Hsieh
778 C. F., Huang T. C. , Ohashi H., Yang Y. P and Lu S. Y.. Taipei, Taiwan: Editorial Committee of
779 *Flora of Taiwan*; 114–115, 122, 1996.
780

781 Liew P.-M., Huang S.-Y. and Kuo C.-M.: Pollen stratigraphy, vegetation and environment of the
782 last glacial and Holocene—A record from Toushe Basin, central Taiwan. *Quatern Int* 147, 16–
783 33, 2006.
784

785 Liu D., Gao X., Wang X., Zhang S., Pei S. and Chen F.: Palaeoenvironmental changes from
786 sporopollen record during the later Late Pleistocene at Shuidonggou locality 2 in Yinchuan,
787 Ningxia. *Journal of Palaeogeography*, 13, 4, 467-472 (in Chinese with English abstract), 2011.
788

789 López-Pujol J., Zhang F.-M., Sun H.-Q., Ying T.-S. and Ge S.: Mountains of southern China as
790 “Plant Museums” and “Plant Cradles”: evolutionary and conservation insights. *Mountain*
791 *Research and Development* 31, 3: 261-269, 2011.
792

793 Lu H.-Y., Liu J.-Q., Chu G.-Q., Gu Z.-Y., Negendank J., Schettler G. and Mingram J.: A study of
794 pollen and environment in the Huguangyan maar lake since the last glaciation. *Acta*
795 *Palaeontologica Sinica* 42, 2, 284-291, 2003.
796

797 Mikolajewicz, U., Vizcaino, M., Jungclaus, J., and Schurgers, G.: Effect of ice sheet interactions in
798 anthropogenic climate change simulations, *Geophys. Res. Lett.*, 34, L18706,
799 doi:10.1029/2007GL031173, 2007.
800

801 Milne R. I. and Abbott R. J.: The Origin and Evolution of Tertiary Relict Floras. *Advances in*
802 *Botanical Research* Vol. 38: 281-314, 2002.
803

804 Mix A. C., Bard E. and Schneider, R.: Environmental processes of the ice age: land, oceans,
805 glaciers (EPILOG), *Quaternary Sci. Rev.*, 20, 627–657, 2001.
806

807 Molavi-Arabshahi M., Arpe K. and Leroy S. A. G.: Precipitation and temperature of the south-west
808 Caspian Sea region during the last 55 years, their trends and teleconnections with large-scale
809 atmospheric phenomena. *International Journal of Climatology*. DOI: 10.1002/joc.4483, 2015.
810

811 Momohara A., Yoshida A., Kudo Y. and Nishiuchi, Okitsu S.: Paleovegetation and climatic
812 conditions in a refugium of temperate plants in central Japan in the Last Glacial Maximum.
813 *Quatern Int* 425, 38-48, 2016.
814

815 Miyoshi N. and Yano N.: Late Pleistocene and Holocene vegetation history of Ohnuma moor in
816 the Chugoku Mountains, western Japan. *Rev Palaeobot Palyno* 46, 355-376, 1986.
817

818 Nakagawa T., Tarasov P.E., Nishida K., Gotanda K. and Yasuda Y.: Quantitative pollen-based
819 climate reconstruction in central Japan: application to surface and Late Quaternary spectra.
820 *Quaternary Science Reviews* 21, 2099–2113, 2002.
821

822 Ni J., Yu G., Harrison S.P. and Prentice I.C.: Palaeovegetation in China during the late Quaternary:
823 biome reconstructions based on a global scheme of plant functional types. *Palaeogeogr.*
824 *Palaeoclimatol. Palaeoecol.* 289, 44–61, 2010.
825

826 Ni J., Cao X., Jeltsch F. and Herzschuh U.: Biome distribution over the last 22,000 yr in China.
827 *Palaeogeogr, Palaeocl* 409, 33–47, 2014.
828

829 Nishiuchi R., Momohara A., Osato S. and Endo K: Temperate deciduous broadleaf forest dynamics
830 around the last glacial maximum in a hilly area in the northern Kanto district, central Japan.
831 *Quatern Int* 455: 113-125, 2017.
832

833 Orain R., Lebreton V., Russo Ermolli E., Combourieu-Nebout N. and Sémah A.-M.: *Carya* as
834 marker for tree refuges in southern Italy (Boiano basin) at the Middle Pleistocene. *Palaeogeogr,*
835 *Palaeocl* 369, 295–302, 2013.
836

837 Park J.: A modern pollen–temperature calibration data set from Korea and quantitative temperature
838 reconstructions for the Holocene. *The Holocene*, 21 (7) 1125–1135, 2011.
839

840 Park J. and Park J.: Pollen-based temperature reconstructions from Jeju island, South Korea and its
841 implication for coastal climate of East Asia during the late Pleistocene and early Holocene.
842 *Palaeogeogr, Palaeoclimatol* 417, 445–457, 2015.

843

844 Piggott D.: *Lime-trees and Basswoods: A Biological Monograph of the Genus Tilia*. 395pp.
845 Cambridge University Press, Cambridge, UK, 2012.

846

847 Qi XS, Yuan N, Comes HP, Sakaguchi S, and Qiu YX: A strong ‘filter’ effect of the East China
848 Sea land bridge for East Asia’s temperate plant species: inferences from molecular
849 phylogeography and ecological niche modelling of *Platycodon grandiflorus* (Malvaceae). *BMC*
850 *Evolutionary Biology*, 14:41, 2014.

851

852 Qian H. and Ricklefs RE: Large-scale processes and the Asian bias in species diversity of
853 temperate plants. *Nature* 407: 180-182, 2000.

854

855 Qiu Y.X., Fu C.X. and Comes HP.: Plant molecular phylogeography in China and adjacent
856 regions: Tracing the genetic imprints of Quaternary climate and environmental change in the
857 world’s most diverse temperate flora. *Molecular Phylogenetics and Evolution* 59, 225–244,
858 2011.

859

860 Reichler, T., and J. Kim: How Well do Coupled Models Simulate Today's Climate?
861 *Bull. Amer. Meteor. Soc.*, 89, 303-311, 2008.

862

863 Roche D. M., Dokken T. M., Goosse H., Renssen H., and Weber S. L.: Climate of the last glacial
864 maximum: sensitivity studies and model-data comparison with the LOVECLIM coupled model.
865 *Clim. Past*, 3, 205-224, 2007.

866

867 Roeckner, E., Bäuml, G., Bonaventura, L., Brokopf, R., Esch, M., Giorgetta, M., Hagemann, S.,
868 Kirchner, I., Kornbluh, L., Manzini, E., Rhodin, A., Schlese, U., Schulzweida, U., and
869 Tompkins, A.: The atmospheric general circulation model ECHAM5, Part I: Model description,
870 Max Planck Institute for Meteorology, Hamburg, Report no. 349, 2003.

871

872 Schneider U., Becker A., Finger P., Meyer-Christoffer A., Rudolf B. and Ziese M.: GPCC Full
873 Data Reanalysis Version 6.0 at 0.5: Monthly Land-Surface Precipitation from Rain-Gauges
874 built on GTS-based and Historic Data. DOI: 10.5676/DWD_GPCC/FD_M_V6_050, 2011.

875

876 Shen C., Tang L., Wang S., Li C. and Liu K.: The Pollen Records and time scale from the RM of
877 the Zoige Basin, northeastern Qinghai-Tibetan Plateau. Chinese Science Bulletin, 50, 6, 553-
878 562, 2005.

879

880 Sitch S., Smith B., Prentice I. C., Arneth A., Bondeau A., Cramer W., Kaplan J.O., Levis S., Lucht
881 W., Sykes M. T., Thonicke K. and Venevsky S.: Evaluation of ecosystem dynamics, plant
882 geography and terrestrial carbon cycling in the LPJ Dynamic Global Vegetation Model. *Global*
883 *Change Biology* 9, 161-185, 2003.

884

885 Shimada M., Takahara H., Imura R., Haraguchi T., Yonenobu H. I. Hayashida A. and Yamada K.:
886 Vegetation history based on pollen and charcoal analyses since the Last Glacial Maximum in
887 southern Kyushu, Japan. EPPC Padua Italy 26-21 August 2014, abstract book p. 253, 2014.

888

889 Solla A., Martin JA and Corral P, Gil L.: Seasonal changes in wood formation of *Ulmus pumila*
890 and *U. minor* and its relation with Dutch elm disease. *New Phytologist* 166, 1025-1034, 2005.

891

892 Sugaya M., Okuda M. and Okada M.: Quantitative paleoclimate reconstruction based on a 130 ka
893 pollen record from teC9001C core off NE Japan. *Quatern Int* 397, 404-416, 2016.
894

895 Sun X. J., Song C. Q. and Wang F. Y.: Vegetation history of the Southern Loess Plateau of China
896 during the last 100,000 years based on pollen data. *Acta Botanica Sinica*, 38, 12, 982-988. (in
897 Chinese with English summary), 1996.

898

899 Sun X.J. and Li X.: A pollen record of the last 37 ka in deep sea core 17940 from the northern
900 slope of the South China Sea. *Marine Geology*, 156, 227-244. 1999.
901

902 Sun X., Li X., Luo Y. and Chen X.: The vegetation and climate at the last glaciation on the
903 emerged continental shelf of the South China Sea. *Palaeogeogr, Palaeocl* 160, 301–316, 2000.
904

905 Sun X., Luo Y, Huang F., Tian J. and Wang P.: Deep-sea pollen from the South China Sea:
906 Pleistocene indicators of East Asian monsoon. *Marine Geology* 201, 97-118, 2003.
907

908 Svenning J.-C.: Deterministic Plio-Pleistocene extinctions in the European cool-temperate tree
909 flora. *Ecology Letters*, 6: 646–653, 2003.
910

911 Takahara H. and Takeoka M.: Vegetational changes since the last Glacial maximum around the
912 Hatchodaira Moor, Kyoto, Japan. *Japan Journal Ecology* 36, 105-116, 1986.
913

914 Takahara H. and Takeoka M.: Vegetation history since the last glacial period in the Mikata
915 lowland, the Sea of Japan area, western Japan. *Ecological Research* 7, 371-386, 1992.

916 Takahara Hi, Sugita S., Harrison S.P., Miyoshi N., Morita Y. and Uchiyama T.: Pollen-based
917 reconstructions of Japanese biomes at 0, 6000 and 18,000 14C yr BP. *J Biogeogr*, 27, 665–683,
918 2000.

919 Tian Z. and Jiang D.; Revisiting last glacial maximum climate over China and East Asian monsoon
920 using PMIP3 simulations. *Palaeogeography, Palaeoclimatology, Palaeoecology* 453 115–126,
921 2016.

922 Tian B, Liu R., Wang L., Qiu Q., Chen K. and Liu J.: Phylogeographic analyses suggest that a
923 deciduous species (*Ostryopsis davidiana* Decne., Betulaceae) survived in northern China during
924 the Last Glacial Maximum. *J Biogeogr* 36, 2148–2155., 2009.

925

926 Tian F., Cao X., Dallmeyer A., Ni J., Zhao Y., Wang Y. and Herzschuh U.: Quantitative woody
927 cover reconstructions from eastern continental Asia of the last 22 kyr reveal strong regional
928 peculiarities. *Quatern Sci Rev*, 137, 33-44, 2016.

929

930 Tian Z. and Jiang D.: Revisiting last glacial maximum climate over China and east Asian monsoon
931 using PMIP3 simulations. *Palaeogeogr, Palaeocl, Palaeocol* 453, 115-126, 2016.

932

933 Wang S., Lu H., Han J., Chu G., Liu J. and Negendank J. F. W.: Palaeovegetation and
934 palaeoclimate in low-latitude southern China during the Last Glacial Maximum. *Quatern Int*
935 248, 79-85, 2012.

936

937 Willis KJ. and Niklas KJ.: The role of Quaternary environmental change in plant macroevolution:
938 the exception or the rule? *Phil. Trans. R. Soc. Lond. B* 359, 159–172. 2004.

939

940 Wu G., Qin J., Deng B. and Li C.: Palynomorphs in the first paleosol layer in the Yangtze Delta
941 and their paleoenvironmental implication. *Chinese Science Bulletin*. 47, 21, 1837-1842, 2002.

942

- 943 Xu D., Lu H, Wu N and Liu Z.: 30 000-Year vegetation and climate change around the East China
944 Sea shelf inferred from a high-resolution pollen record. *Quatern Int* 227, 53-60, 2010.
945
- 946 Xu G., Yang X., Ke Z., Li Nag W. and Yang Z.: Environment Changes in Yanshan Mountain
947 Area during the Latest Pleistocene. *Geography and Territorial Research*, 18, 2, 4 pages, 2002.
948
- 949 Yan G., Wang F.B., Shi G.R. and Li S.F.: Palynological and stable isotopic study of
950 palaeoenvironmental changes on the northeastern Tibetan plateau in the last 30,000 years.
951 *Palaeogeogr, Palaeoclim, Palaeocl* 153, 147–159, 1999.
952
- 953 Yang D., Peng Z., Luo C., Liu Y., Zhang Z., Liu W. and Zhang P.: High-resolution pollen
954 sequence from Lop Nur, Xinjiang, China: Implications on environmental changes during the
955 late Pleistocene to the early Holocene. *Palaeobot Palyno* 192, 32–41, 2013.
956
- 957 Yi S. and Kim S.-J.: Vegetation changes in western central region of Korean Peninsula during the
958 last glacial (ca. 21.1–26.1 cal kyr BP). *Geosci J* 14, 1, 1 – 10, 2010.
959
- 960 Yu S, Zheng Z., Chen Z, Jing X, Kershaw P., Moss P., Peng X., Zhang X., Chen C., Zhou Y.,
961 Huang K. and Gan H.: A last glacial and deglacial pollen record from the northern South China
962 Sea: New insight into coastal-shelf paleoenvironment. *Quatern Sci Rev* 157, 114-128, 2017.
963
- 964 Yu G., Ke X., Xue B. and Ni J.: The relationships between the surface arboreal pollen and the
965 plants of the vegetation in China. *Palaeobot Palyno* 129, 187– 198, 2004.
966
- 967 Yue Y., Zheng Z., Huang K., Chevalier M., Chase B. M., Carré M., Ledru M.-P. and Cheddadi R.:
968 A continuous record of vegetation and climate change over the past 50,000 years in the Fujian

969 Province of eastern subtropical China. *Palaeogeogr, Palaeoclimatol* 365–366:115–123, DOI:
970 10.1016/j.palaeo.2012.09.018, 2012.

971

972 Zheng Z., Huang K., Deng Y., Cao L., Yu S., and Suc J.-P.: A 200 ka pollen record from Okinawa
973 Trough: Paleoenvironment reconstruction of glacial-interglacial cycles. *Science China Earth*
974 *Sciences* 56 (10), 1731-1747, 2013.

975

976 Zheng Z., Wei J., Huang K., Xu Q., Lu H., Tarasov P., Luo C., Beaudouin C., Deng Y., Pan A.,
977 Zheng Y., Luo Y., Nakagawa T., Li C., Yang S., Peng H. and Cheddadi R.: East Asian pollen
978 database: modern pollen distribution and its quantitative relationship with vegetation and
979 climate. *J Biogeogr.* doi:10.1111/jbi.12361, 2014.

980

981 Ziska, L. H. and Caulfield, F. A.: Rising CO₂ and pollen production of common ragweed
982 (*Ambrosia artemisiifolia*), a known allergy inducing species: implications for public health,
983 *Aust. J. Plant Physiol.*, 27, 893–898, 2000,

984

985

986 **BIOSKETCH**

987 Suzanne Leroy is a physical geographer, specialised in palynology. She works at various time scales and
988 resolutions from the Pliocene to the present in the Mediterranean basin, NW Africa and SW Asia as well as
989 further to the east (Kyrgyzstan and NE China), always in a multidisciplinary way, mostly in cooperation with
990 geologists and archaeologists for understanding past environments and climates, the origin of sediments, and
991 the interactions between nature and humans. Although the analysed sediments were mostly lacustrine,
992 additional experiences are in marine and deltaic environments. Recently she developed an interest in
993 phylogeography and environmental catastrophes.

994 Author contributions: S.L. is responsible for the overall research and collected the pollen data with help by
995 J.W., K.A. is responsible for the meteorology and climatology aspects as well as did most of the

996 programming and writing of the manuscript, U.M. provided the climate model simulations and J.W.
997 contributed to the data search and typical Chinese aspects.
998